1951

Connections for welded continuous portal frames part 2, Progress Report 4, theoretical analysis of straight knees

A. A. Topractsoglou

L. S. Beedle

B. Johnston

REPORT NO. 205C.5B$_2$
DATE 3-31-51

FRITZ ENGINEERING LABORATORY
LEHIGH UNIVERSITY
REPORT

CONNECTIONS FOR WELDED CONTINUOUS PORTAL FRAMES

XXX

PART II

"Theoretical Analysis of Straight Knees"

BY

A.A. Topractsoglou, Lynn S. Beedle, Bruce G. Johnston

Type 8B

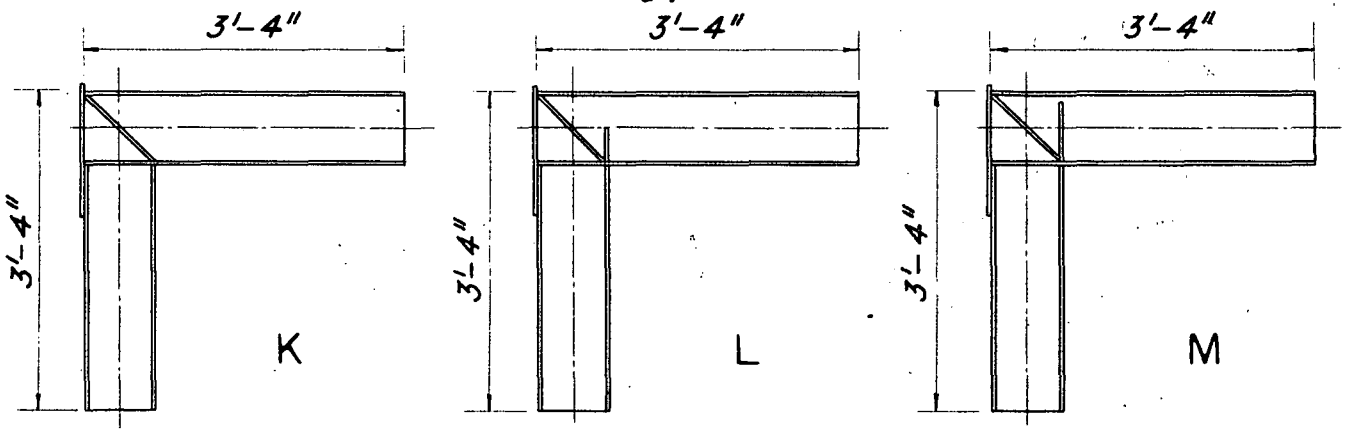

Type 7

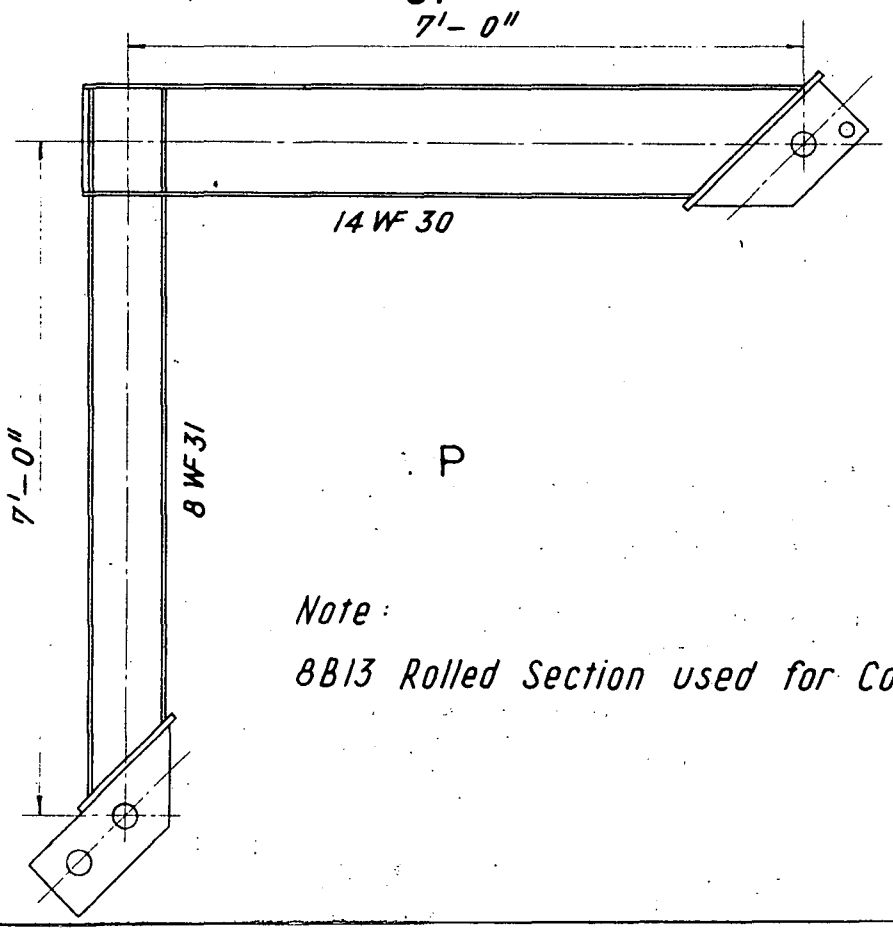

Type 2

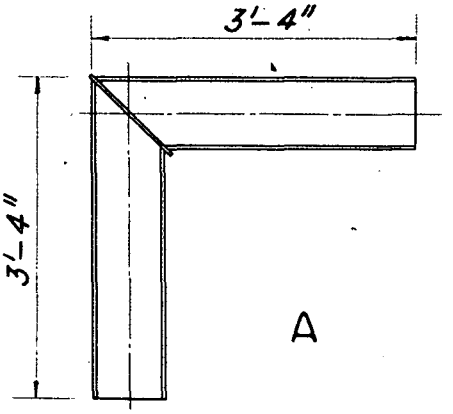

Note:

8B13 Rolled Section used for Connections A-N.

Welded Continuous Frames and Their Components

Progress Report 4

CONNECTIONS FOR WELDED CONTINUOUS PORTAL FRAMES

(Part II)

Section V: "Theoretical Analysis of Straight Knees"

By

A.A. Topractsoglou, Lynn S. Beedle, Bruce G. Johnston

This work has been carried out as a part of an investigation sponsored jointly by the Welding Research Council and the Department of the Navy with funds furnished by the following:

American Institute of Steel Construction
American Iron and Steel Institute
Column Research Council (Advisory)
Institute of Research, Lehigh University
Office of Naval Research (Contract No. 39303)
Bureau of Ships
Bureau of Yards and Docks

Fritz Engineering Laboratory
Department of Civil Engineering and Mechanics
Lehigh University
Bethlehem, Pennsylvania

March 31, 1951

Fritz Laboratory Report No. 205C.6B

TABLE OF CONTENTS

Foreword To Part II

Part I of this report was completed and distributed under date of December 7, 1950. It was indicated there that the theoretical analysis of square knees* was to be presented separately as "Part II" for criticism by members of the Lehigh Project Subcommittee, Welding Research Council.

Part II has now been completed and will be followed at a later time by Part III which will include the discussion of test results, conclusions and acknowledgements. The comparison of experimental results with the theoretical values developed here is also included in Part III. However, the figures included at the end of Part II afford an immediate basis for comparison.

Figure numbers are either the same as used in the dissertation upon which this work is based or are extensions of the sequence. This accounts for the large numbers, which will be modified in the published version. Most of the dissertation figures referred to in this section have been reproduced here. The list of references contained in Part I has not been duplicated.

- -

* The terms "square" and "straight" are both used to designate a connection in which the girder and column rolled sections are joined at right angles without the use of additional haunch or bracket material.

PART II

Theoretical Analysis of Straight Knees

I E L A S T I C A N A L Y S I S

F. Bleich[37] has proposed approximate methods for stress analysis and design of square knees. He assumes that for square knees:

> "... where the ratio of the length of the restraining arm to its depth is equal to or larger than one, the Navier theory yields sufficiently accurate results and one may determine the fibre stresses and shear stresses according to the conventional theory."

By "restraining arm" is meant the arm AD, which acts to restrain the girder, Fig. 140*

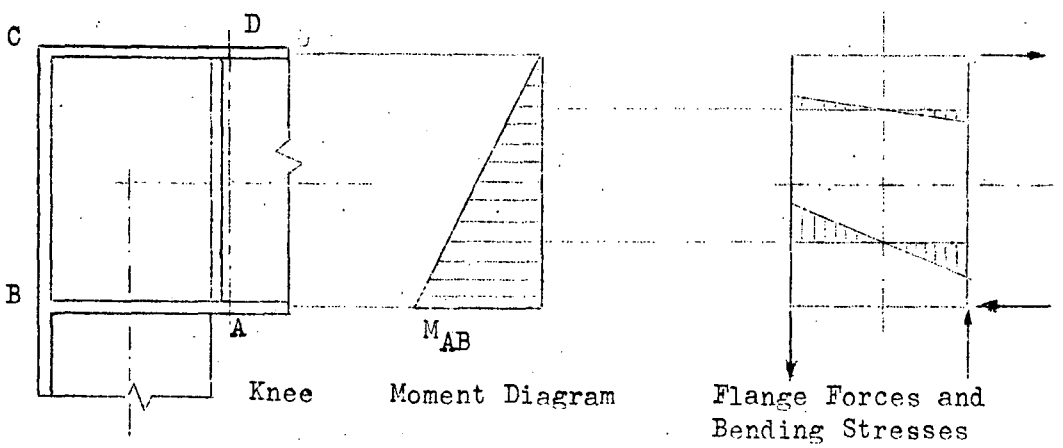

Fig. 140

---

* Concerning the figure numbers, see the Foreword.

In the rolled section adjacent to the knee (at section AD) it has also been assumed that the ordinary beam theory applies for predicting stresses and deformations.

1. STRESS ANALYSIS OF STRAIGHT KNEES WITHOUT DIAGONAL STIFFENERS (Types 3, 7 and 8)

1a. Identical Rolled Shapes:

Consider the type 7 connection shown in Fig. 13(a)*. The stresses in the knee ABCD are found by making the following assumptions:

(1) The bending moment at the section AD is taken entirely by the flanges. In the knee shown, $M_r = V(L - \frac{d}{2})$ and the portion of the flange force, F, due to bending is given by

$$F = \frac{M_r}{d} = V(\frac{L}{d} - \frac{1}{2})$$

The designation M_r will be used throughout this report to indicate the moment at the end of the rolled section and beginning of the knee, whether it be straight, curved or haunched. M_h is then used to denote the "haunch" moment or moment at the intersection of the neutral lines of the girder and column. In the above expression the remaining terms are defined by Fig. 13.

---

* This figure is duplicated at the back of this report.

(2) Shear, V, is taken by the web and is uniformly distributed.

(3) The normal force N, is considered. It is assumed to act at the flanges, however, as shown in Fig. 141.

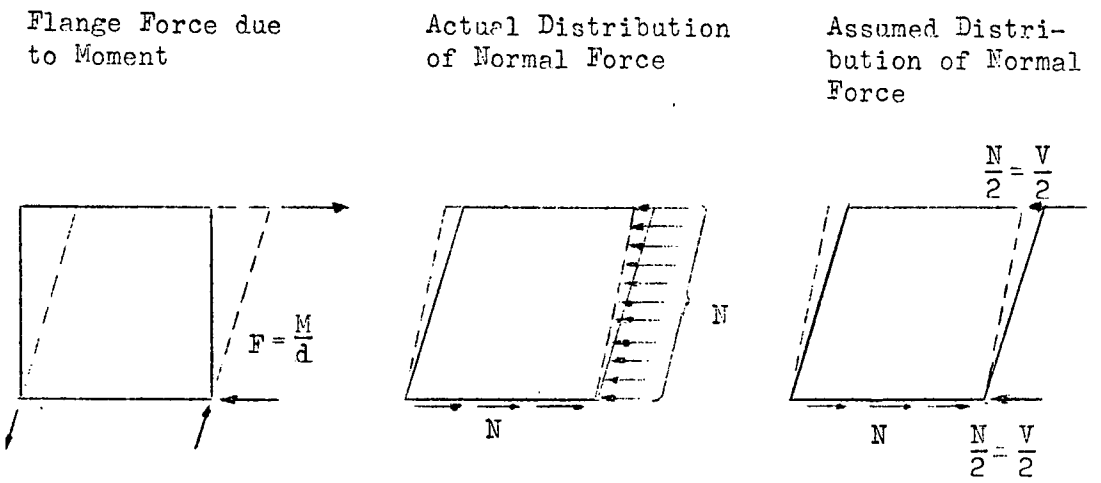

Fig. 141

(4) The flange force varies with a straight-line variation between D and C, with maximum at D and zero at C.

(5) Stress concentrations are not considered.

(6) Normal stress is assumed to vary linearly throughout depth of knee.

(7) Restraint due to bending of individual flange elements is neglected.

Fig. 13c shows the forces acting on the knee. Taking into account the above assumptions, the forces and stresses are applied to the flange element as shown in Fig. 142(a). Stresses on the web are indicated in Fig. 142(b).

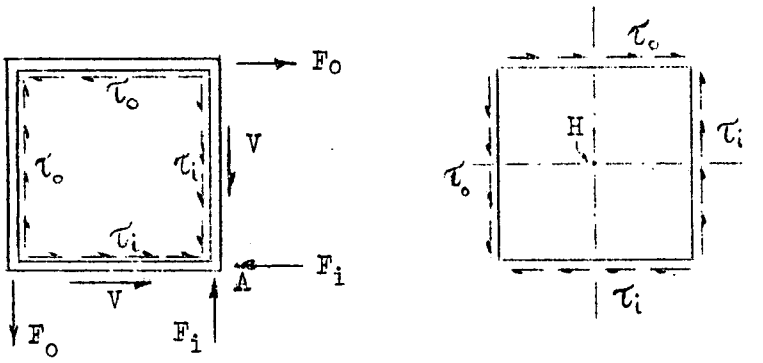

(a) Forces and Stresses on Flanges

(b) Stresses on Web

Fig. 142

Subscripts o and i represent "outside" and "inside" forces or stresses, respectively. Neglecting the web and noting that N = V, the outside flange force is given by

$$F_o = \frac{M_r}{d} - \frac{N}{2}$$

$$F_o = \frac{V(L-d/2)}{d} - \frac{V}{2}$$

$$F_o = V\left(\frac{L}{d} - 1\right)$$

At the inside flange,

$$F_i = \frac{M_r}{d} + \frac{V}{2} = \frac{V\left(L-\frac{d}{2}\right)}{d} + \frac{V}{2}$$

$$F_i = \frac{VL}{d}$$

Computing the shear stresses τ on the web panel,

$$\tau_o = \frac{F_o}{A_w} = \frac{V}{A_w}\left(\frac{L}{d} - 1\right)$$

where

A_w = area of the web.

Then

$$\tau_i = \frac{F_i - V}{A_w} = \frac{V\frac{L}{d} - V}{A_w}$$

$$\tau_i = \frac{V}{A_w}\left(\frac{L}{d} - 1\right) \quad \ldots\ldots\ldots\ldots\ldots\ldots\ldots \quad (1)$$

Thus

$$\tau_o = \tau_i$$

The stress distributions in the various elements are as follows:

(1) The knee web is loaded in pure shear (Fig. 142b)

(2) The stresses in the flanges forming the knee are distributed as shown in Fig. 143(a).

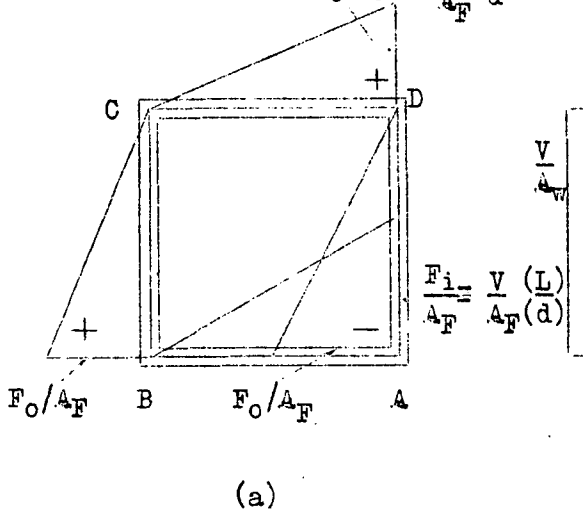

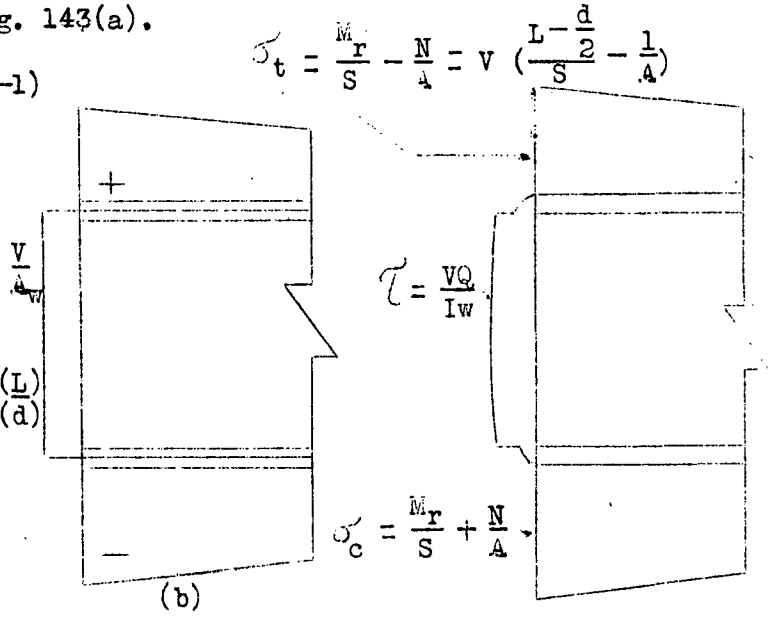

Fig. 143 Fig. 144

(3) To the right of section AD, the stresses are given by Fig. 143(b).

---

* Ordinate represents mean horizontal normal stress in beam flange cross-section. Tensile stresses are ploted external to the knee.

The stress distributions shown in Fig. 144 correspond to those of Fig. 143(b) except that they are computed on the basis of ordinary beam theory. Comparing the resulting stresses at section AD for a connection with 14WF30 members indicates a difference of about 8% which will be neglected.

The theoretical stresses may be compared to experimentally-determined values on the basis of either load or moment. The latter will be used hereafter.

From the point of view of balanced design the shear stress at point H of Fig. 142 should reach the yield value at the same external bending moment at which point A reaches the yield point in combined bending and direct stress. (Actual combined stresses will be higher elsewhere, but for engineering purposes it is considered that examination of the separate stresses at these two points is adequate.)

The stress patterns at other places in the connections were measured and a later paper will present the results as compared with the theoretically-predicted values.

It is of importance that yielding due to shear force does not occur in unstiffened knee webs below the flexural yield load. Such yielding may cause large deformations. Conventional design neglects the possibility of such shear deformation and it is not practical to attempt to take it into account in routine deformation computations. Therefore, the investigation of yielding in an

unstiffened knee web (types 3, 7 and 8)* is of importance.

Given the square knee loaded as described previously, the problem is to find the moment under which yielding due to shear force occurs in the web.

According to the assumptions used herein, shear stresses in the knee web are uniform along horizontal sections. The actual bending stresses at section DA (Fig. 143a) cause maximum shearing stresses to occur at point H, decreasing toward the flanges. This maximum value is somewhat greater than the average uniform value, but this increase is neglected for the time being.

The following values will be substituted into Eq. (1):

$$A_w = d \times w$$

and

$$V = \frac{M_h}{L}$$

Thus

$$\tau = \frac{M_h}{wd^2}\left(1 - \frac{d}{L}\right)^{**} \quad \ldots\ldots\ldots\ldots\ldots\ldots \quad (2)$$

Since the normal stresses are negligible at the center of the knee, a state of pure shear may be assumed, and

$$\sigma_1 = -\sigma_2 = \tau$$

---

* Knee types are shown on the inside of front cover.

** For connection P, $\frac{d}{L} = \frac{13.75}{84} = .164$, $\left(1 - \frac{d}{L}\right) = .836$

For connections A,L, $\frac{d}{L} = \frac{8.06}{36} = .224$, $\left(1 - \frac{d}{L}\right) = .786$

Thus the web yields when the maximum shear stress equals

$$\tau_y = \frac{\sigma_y^*}{2}$$

in which σ_y = lower yield point stress of web material as determined in a simple tension test. Thus from Eq. (2), substituting for τ the value $\sigma_y/2$,

$$M_{h(\tau)} = \frac{\sigma_y \, wd^2}{2\,(1-d/L)} \quad \ldots\ldots\ldots\ldots\ldots\ldots \quad (3)$$

where $M_{h(\tau)}$ is the moment at which yielding occurs due to shear force in the web (point H, Fig. 142b).

The stress at point A, Fig. 142, is given by

$$\sigma_c = \frac{M_r}{S} + \frac{N}{A} = \frac{M_r}{S} + \frac{V}{A}$$

Since

$$M_h = VL,$$

and

$$M_r = M_h\,(1 - \frac{d}{2L}),$$

then

$$\sigma_c = M_h \frac{(1 - \frac{d}{2L})}{S} + \frac{1}{AL}$$

$$M_{h(\sigma)} = \frac{\sigma_y}{\frac{(1-\frac{d}{2L})}{S} + \frac{1}{AL}} \quad \ldots\ldots\ldots\ldots\ldots\ldots \quad (4)$$

in which $M_{h(\sigma)}$ is the moment at the haunch when yielding occurs due to flexure and direct stress at the critical section DA.

---

* The maximum shear stress theory is conservative. More accurately, by the octahedral shear stress theory, $\tau_y = .578\sigma_y$

If the ratio $\frac{M_{h(\tau)}}{M_{h(\sigma)}}$ is formed it will be possible to determine whether a connection fabricated of a particular rolled shape will yield in the web (shear) or in the rolled shape (flexure). So long as the ratio is greater than 1.0 yielding due to shear force within the knee should not occur.

Then from (3) and (4)

$$\frac{M_{h(\tau)}}{M_{h(\sigma)}} = \frac{\frac{\sigma_y\, wd^2}{2\,(1-d/L)}}{\sigma_y} \times \frac{1-\frac{d}{2L}}{S} + \frac{1}{AL}$$

$$\frac{M_{h(\tau)}}{M_{h(\sigma)}} = \frac{wd^2}{2(1-\frac{d}{2L})}\left\{\frac{(1-\frac{d}{2L})}{S} + \frac{1}{AL}\right\} \quad \ldots\ldots\ldots\ldots\ldots (5)$$

Some commonly-available rolled sections have been investigated using Eq. (5). The results given in Table 1 show that in square knees with no diagonal stiffener yielding normally takes place in the web.

TABLE I

Section (1)	S (2)	w (3)	d (4)	A (5)	$\frac{M_{h(\tau)}}{M_{h(\sigma)}}$ ($L/d=6.0$) (6)	$\frac{M_{h(\tau)}}{M_{h(\sigma)}}$ ($L=L_u$) (7)
14WF30	41.8	.270	13.90	8.81	.726	0.928
8B13	9.88	.230	8.00	3.83	.867	0.822
21WF82	168	.499	20.86	24.10	.754	-
6B12	7.24	.230	6.00	3.53	.666	-
24WF110	274.4	.510	24.16	32.36	.633	-
8WF31	27.4	.288	8.00	9.12	.517	0.364

The calculation in Table I shows that "shear yielding" will usually occur prior to yielding in flexure (based on a constant L/d ratio of 6.0) An alternate basis for comparison would be obtained if the value "L_u" were selected such that Ld/bt = 600 ...

a limiting case for lateral buckling. Three examples were selected and the resulting ratio is shown in column 7. The same general result is obtained. Note that the 8WF31 "column" section is particularly deficient.

1b. Stress Analysis: Dissimilar Rolled Shapes ($d_1 \neq d_2$)

Reference is made to Fig. 145 and the assumptions stated earlier. It will be further assumed that $d_2 < d_1$. The subscripts 1 and 2 refer to members 1 and 2.

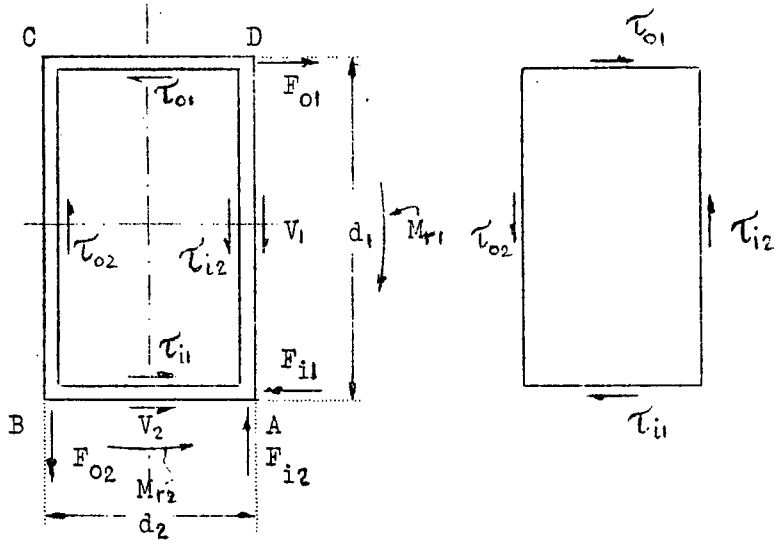

(a) (b)

Fig. 145

Then

$$F_{o1} = \frac{M_{r1}}{d_1} - \frac{V}{2}$$

$$M_{r1} = V\left(L - \frac{d_2}{2}\right)$$

$$F_{o1} = \frac{V}{d_1}\left[L - \frac{(d_1 + d_2)}{2}\right] \quad \text{..... (6)}$$

Also

$$F_{i1} = \frac{M_{r1}}{d_1} + \frac{V}{2}$$

$$F_{i1} = \frac{V}{d_1}\left[L + \frac{(d_1 - d_2)}{2}\right] \quad \text{..... (7)}$$

Similarly,

$$\left.\begin{aligned} F_{o2} &= \frac{V}{d_2}\left[L - \frac{(d_1+d_2)}{2}\right] \\ F_{i2} &= \frac{V}{d_2}\left[L + \frac{(d_2-d_1)}{2}\right] \end{aligned}\right\} \quad \text{..... (8)}$$

Since

$$\tau = \frac{F}{A_w}$$

$$\tau_{o1} = \frac{F_{o1}}{wd_2} = \frac{V}{wd_1d_2}\left[L - \frac{(d_1+d_2)}{2}\right]$$

$$\tau_{i1} = \frac{F_{i1}-V}{wd_2} = \frac{V}{wd_1d_2}\left[L + \frac{(d_1-d_2)}{2}\right] - \frac{V}{wd_2} = \frac{V}{wd_1d_2}\left[L - \frac{(d_1+d_2)}{2}\right]$$

$$\tau_{o2} = \frac{F_{o2}}{wd_1} = \frac{V}{wd_1d_2}\left[L - \frac{(d_1+d_2)}{2}\right]$$

$$\tau_{i2} = \frac{F_{i2}-V}{wd_1} = \frac{V}{wd_1d_2}\left[L + \frac{(d_2-d_1)}{2}\right] - \frac{V}{wd_1} = \frac{V}{wd_1d_2}\left[L - \frac{(d_1+d_2)}{2}\right]$$

All the τ's are equal and the web, neglecting small bending effects, is in a state of pure shear,

$$\tau = \frac{V}{wd_1d_2}\left[L - \frac{(d_1+d_2)}{2}\right] \quad \ldots\ldots\ldots\ldots\ldots\ldots \quad (9)$$

Then

$$\tau = \frac{M_h}{wd_1d_2}\left[1 - \frac{(d_1+d_2)}{2L}\right] \quad \ldots\ldots\ldots\ldots\ldots\ldots \quad (10)$$

To investigate initial yield in the web due to shear force and in the flange due to bending, assume first, that member "2" is weaker than member "1" and that flexural yield will occur at point A on section AB in Fig. 145. Yield due to shear force occurs when

$$\tau = \frac{\sigma_y}{2}$$

Therefore, from Eq. (10),

$$M_{h(\tau)} = \frac{wd_1d_2\,\sigma_y}{2}\left(\frac{1}{1 - \frac{d_1-d_2}{2L}}\right)^{*} \quad \ldots\ldots\ldots\ldots\ldots\ldots \quad (11)$$

At point A, from Eq. (4),

$$\sigma_y = \frac{M_{r2}}{S_2} + \frac{V}{A_2} = \frac{M_{r2}}{S_2} + \frac{M_h}{A_2L}$$

---

* It is evident from this expression that the member with the thickest web should be made continuous into the knee so that the greater thickness of web will assist in carrying the shear force.

$$\sigma_y = M_h \frac{1-d_1/2L}{S_2} + \frac{1}{A_2 L}$$

$$M_{h(\sigma)} = \frac{\sigma_y}{\frac{(1-d/2L)}{S_2} + \frac{1}{A_2 L}} \quad \text{..... (12)}$$

Applying expressions (11) and (12) to connection test P (type 7 knee using 8WF31 and 14WF30 shapes) and using the dimensions and properties determined from the specimens (Appendix 1),

$$M_{h(\tau)} = 724 \text{ in-kips}$$

$$M_{h(\sigma)} = 1140 \text{ in-kips}$$

The magnitude of $M_{h(\tau)}$ is plotted as a horizontal line in Fig. 38.

The ratio of the two moments is

$$\frac{M_{h(\tau)}}{M_{h(\sigma)}} = \frac{724}{1170} = 0.619$$

Comparing this result with the calculations of Table I, it is evident that the worst case is that in which the two section depths are not equal (compare 0.726 with 0.619).

Earlier in this report it was assumed that the shear stress was uniformly distributed across the web. However, according to F. Bleich's original assumption, shear stresses would be distributed in parabolic form. Thus,

$$\tau_{max} = \frac{V_k Q_k}{I_k t_k} \quad \text{..... (13)}$$

where the subscripts, k, denote dimensions in the knee, Q_k is the static moment of one-half the cross-section and t_k is the stiffener thickness. Since, from Fig. 145,

$$V_k = F_{o1},$$

then from Eqs. (13), (6), and (9),

$$\frac{\tau_{max}}{\tau_{ave}} = \frac{Q_k d_2}{I_k} \quad \ldots\ldots\ldots\ldots\ldots\ldots \quad (14)$$

For test connection P,

$$\frac{\tau_{max}}{\tau_{ave}} = 1.15$$

or the maximum shear at point H is 15% greater than the average value computed according to Eq. (9). The more accurate predicted value for $M_{h(\tau)}$ is then,

$$M_{h(I)} = \frac{724}{1.15} = 630 \text{ in-kips}$$

which gives better agreement with the experimentally-determined value. The previous expressions for "shear" yielding could all be modified by an appropriate factor $\frac{Q_k d_k}{I_k}$. However, since this would have the effect of decreasing the ratio $\frac{M_{h(\tau)}}{M_{h(\sigma)}}$ in Table I, which values are already less than unity, the modification only lends further emphasis to the necessity for additional stiffening to prevent undesirable shear deformation.

This analysis can at best only be considered as approximate. First of all the boundary conditions are not exactly as assumed.

When the flanges are thick in proportion to the depth of the section they provide additional restraint which will enable the knee to carry more load before yielding due to shear force commences.

Secondly, residual stress is built up in the knee due to welding of the stiffeners (see Fig. 115, Part I). Presumably this alone would cause yielding to occur at a lower load than predicted.

2. ROTATION ANALYSIS

The knee rotation is made up of two parts:

(1) Rotation due to shear, designated as γ, and

(2) Rotation due to bending, designated as β.

Since a comparison is to be made later with experimentally -determined values there is a third component to be considered:

(3) Rotation due to bending of the rolled section over the length, r, between the knee and point of rotation measurement, designated as ϕ_r.

Therefore, the total knee rotation is

$$\theta = \gamma + \beta + \phi_r \quad \ldots\ldots\ldots\ldots\ldots\ldots \quad (15)$$

2a. Type 7 Connection with Identical Members ($d_1 = d_2$):

The assumptions of section 1a will be used.

From Fig. 13(b) and Eq. (2), the rotation due to shear is,

$$\gamma_7 = \tau/G$$

$$\gamma_7 = \frac{M_h}{wd^2G}\left(1 - \frac{d}{L}\right) \quad \ldots\ldots\ldots\ldots\ldots\ldots \quad (16)$$

Where

γ_7 = shear rotation of type 7 connection

G = shear modulus

The rotation due to bending moment may be determined from the elongations or contractions of the flanges. As stated earlier, it is assumed that the web carries all the shear force and the flange elements carry the direct stresses.

The flange stresses are shown in Fig. 143a. Depending on the boundary conditions assumed, the flanges will deform into one of the patterns shown in Fig. 146.

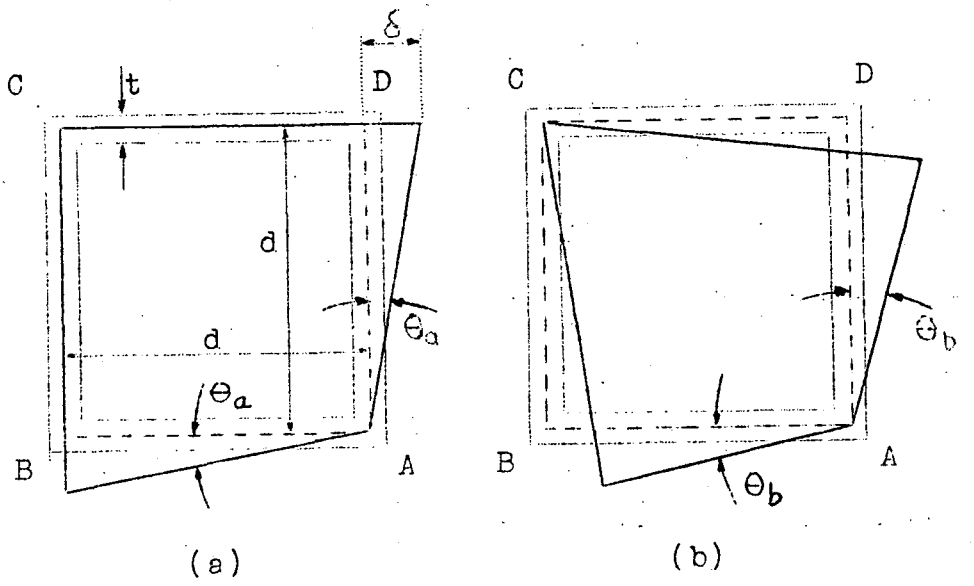

Fig. 146: Flange Deformations

In Fig. 146(a), the tension flanges BC and CD elongate, but the shortening of the compression flange is not considered. In this case $\beta = 2\Theta_a$. In Fig. 146(b), the extension and shortening of all four flanges is considered according to the assumed stress distribution of Fig. 143; then $\beta = 2\Theta_b$. In both Figs. 146(a) and (b) point A does not shift with respect to point C since the rotation resulting

from such motion is included in the shear deformation determined from Eq. (16).

Since all of the extensions and contractions are small quantities, the angle θ_a will very nearly equal θ_b. It will be assumed so; because of its simplicity, the deformation pattern of Fig. 146(a) will also be assumed throughout this report.

Let δ be the extension of the tension flanges BC and CD due to the average flange stress $\frac{\sigma_t}{2}$. Then

$$\delta = \frac{\sigma_t d}{2E}$$

and

$$\theta_a = \frac{\delta}{d} = \frac{\sigma_t}{2E}$$

The total bending rotation at the knee is

$$\beta = 2\theta_a = \frac{\sigma_t}{E}.$$

Neglecting the influence of direct stress,

$$\sigma_t = \frac{M_r \times c}{I_F} = \frac{M_h \left(1 - \frac{d}{2L}\right) \times \frac{d}{2}}{I_F}$$

Then

$$\beta_7 = \frac{M_h \left(1 - \frac{d}{2L}\right) \times d}{2EI_F} \qquad \text{..... (17)}$$

where

$$I_F = 2A_F \left(\frac{d}{2} - \frac{t}{2}\right)^2$$

A_F = flange area

t = flange thickness

The rotation, ϕ_r, due to flexure of the rolled section over lengths

r* is given by

$$\phi_r = 2r \left(\frac{M_r}{EI}\right)$$

$$\phi_r = 2r \frac{M_h}{EI} \left(1-\frac{d}{2L}\right) \quad \ldots\ldots\ldots\ldots\ldots\ldots (18)$$

Then the total rotation from Eq. (15) is given by a summation of the values determined from (16), (17) and (18), or

$$\theta_7 = (\gamma'_7 + \beta_7 + \phi_r)$$

$$\theta_7 = \left[\frac{M_h}{wd^2G} \left(1- \frac{d}{L}\right) + \frac{M_h}{2EI_F} \left(1- \frac{d}{2L}\right) d + \frac{M_h \left(1- \frac{d}{2L}\right) 2r}{EI} \right]$$

$$\theta_7 = M_h \left[\frac{\left(1- \frac{d}{L}\right)}{wd^2G} + \frac{\left(1- \frac{d}{2L}\right)d}{2EI_F} + \frac{\left(1- \frac{d}{2L}\right)2r}{EI} \right] \ldots\ldots\ldots (19)$$

Since the test program did not include a type 7 connection with identical members the calculation will not be carried further.

2b. Type 7 Connection with Dissimilar Members ($d_1 \neq d_2$):

From Eq. (10),

$$\gamma'_7 = \frac{\tau}{G} = \frac{M_h}{wd_1d_2G} \left[1 - \frac{(d_1 + d_2)}{2L} \right] \ldots\ldots\ldots\ldots (20)$$

---

* Some r-distances are shown in Fig. 42.

Fig. 147 shows the flange deformations (corresponding with Fig. 146) which are the basis for computing the bending rotations.

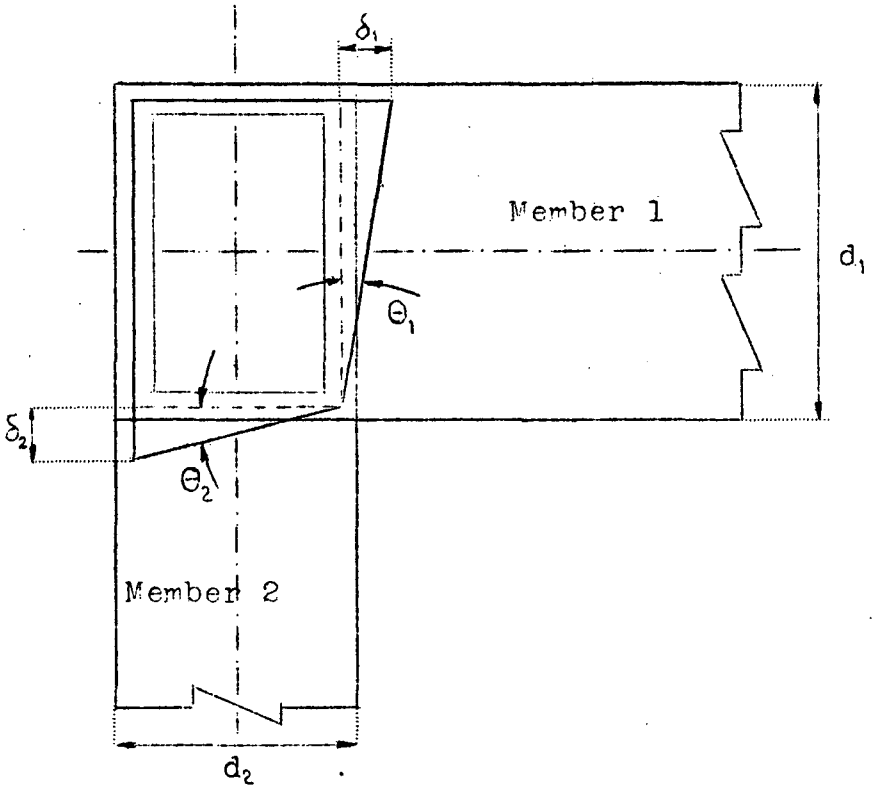

Fig. 147

From the above figure,

$$\beta_7 = \theta_1 + \theta_2$$

$$\theta_1 = \frac{\delta_1}{d_1} = \frac{\sigma_{t1} d_2}{2E d_1}$$

$$\theta_2 = \frac{\delta_2}{d_2} = \frac{\sigma_{t2} d_1}{2E d_2} .$$

Since

$$\sigma_{t1} = \frac{M_h \left(1 - \frac{d_2}{2L}\right) d_1}{2I_{F1}}$$

and

$$\sigma_{t2} = \frac{M_h\,(1-\frac{d_1}{2L})d_2}{2I_{F2}}$$

then

$$\beta_7 = \frac{1}{2E}\left[\frac{d_2\sigma_{t1}}{d_1} + \frac{d_1\sigma_{t2}}{d_2}\right]$$

$$\beta_7 = \frac{M_h}{4E}\left[\frac{(1-\frac{d_2}{2L})d_2}{I_{F1}} + \frac{(1-\frac{d_1}{2L})d_1}{I_{F2}}\right] \qquad \text{.....(21)}$$

The rolled section rotations are computed from

$$\phi_{r1} = r_1\left[\frac{M_h}{EI_1}\,(1-\frac{d_1}{2L})\right]$$

$$\phi_{r2} = r_2\left[\frac{M_h}{EI_2}\,(1-\frac{d_2}{2L})\right]$$

Assuming the r-distances and E-values identical for the two members,

$$\phi_r = \phi_{r1} + \phi_{r2}$$

$$\phi_r = r_1\,\frac{M_h}{E}\left[\frac{(1-\frac{d_1}{2L})}{I_1} + \frac{(1-\frac{d_2}{2L})}{I_2}\right] \qquad \text{..... (22)}$$

Combining Eqs. (20), (21) and (22), the total rotation of a type 7 connection with dissimilar members is given by

$$\theta_r = (\gamma_7 + \beta_7 + \phi_r)$$

$$\theta_7 = M_h\left[\frac{1-\frac{(d_1+d_2)}{2L}}{wd_1d_2G} + \frac{1}{4E}\left\{\frac{(1-\frac{d_2}{2L})d_2}{I_{F1}} + \frac{(1-\frac{d_1}{2L})d_1}{I_{F2}}\right\} + \frac{r_1}{E}\left\{\frac{(1-\frac{d_1}{2L})}{I_1} + \frac{(1-\frac{d_2}{2L})}{I_2}\right\}\right] \qquad \text{..... (23)}$$

Evaluating the total rotation for connection P,

$$\theta_7 = (\gamma_7 + \beta_7 + \phi_r)$$

$$\theta_7 = (2.440 + 1.171 + 0.777) \times 10^{-6} \text{ rad/in-kip}$$

$$\theta_7 = 4.39 \times 10^{-6} \text{ rad/in-kip}$$

This theoretical moment-angle change relationship is plotted with the experimental values in Fig. 38. The relative magnitude of the components γ_7, β_7 and ϕ_r may be seen in the calculation above. The shear component is the largest.

2c. Connections with Diagonal Stiffeners:

(I) TYPE 2 CONNECTIONS

Rotations due to shear in the square knee ABCD reinforced with diagonal stiffeners (Fig. 14) will be found by making the following assumptions:

a. The thrust of the two compressive forces $V_a L/d$ is taken by the stiffener at point A. (See part 1a at the beginning of this section.) The necessity for the designation, V_a, will be described later.

b. The stress on the diagonal stiffener varies linearly from a maximum at A to zero at C. It was assumed earlier that the force, F_o, was transmitted uniformly to the web along the length CD (Fig. 14). A portion of this shear, then, is transmitted to the stiffener in proportion to the length of web intercepted by it.

c. Stress concentrations are disregarded.

From assumption (b) it follows that the stiffener stresses cause uniform shear, τ_s, in the web of the knee. See Fig. 14(b).

The moment required to deform a type 2 connection in shear consists of two parts:

a. the moment necessary to shorten the diagonal stiffener, and

b. that required to deform the web.

Thus the presence of a diagonal reduces the shear stress in the web but a portion of the flange force is transmitted by the web without assistance from the diagonal stiffener.

The total contraction in the diagonal stiffener ΔL_1 is determined from

$$\epsilon = \frac{\sigma}{E} = \frac{\Delta L_1}{\sqrt{2}d}$$

and

$$\Delta L_1 = \frac{\sigma_A}{\sqrt{2}} \frac{d}{E}$$

where

σ_A = stress at point A, Fig. 14

$$\sigma_A = \frac{\sqrt{2}\, F_{ia}}{A_s} = \frac{\sqrt{2}\, V_a L}{A_s d} = \frac{\sqrt{2}\, M_{ha}}{A_s d}$$

A_s = area of diagonal stiffener

and the subscripts "a" relate to the moment associated with contraction of the stiffener. Then

$$\Delta L_1 = \frac{M_{ha}}{A_s E} \qquad \text{.....(24)}$$

Consider the action of the web with the stiffener removed. Due to shearing forces this web will take the shape ABC'D', Fig. 14c. The following relations are then obtained:

$$C'C'' = d_2;\ BC'' = d \sin \gamma_2 \cong d\gamma_2;\ C''A = d(1-\gamma_2),$$

where

γ_2 = the shearing strain in type 2 connections.

The change in length ΔL_2 along the diagonal line AC is given by

$$\Delta L_2 = CA - C'A = d\sqrt{2} - \sqrt{d^2 + d^2(1-\gamma_2)^2}$$

The second term may be expanded as a series, and neglecting terms of higher degree,

$$\Delta L_2 = \frac{\gamma_2 d}{\sqrt{2}} \qquad \text{..... (25)}$$

Since this change in length must be equal to the contraction in the stiffener, then

$$\Delta L_1 = \Delta L_2$$

and from (24) and (25),

$$\frac{M_{ha}}{A_s E} = \frac{\gamma_2 d}{\sqrt{2}}$$

$$M_{ha} = \frac{\gamma_2 A_s E d}{\sqrt{2}} \qquad \text{..... (26)}$$

In considering the second of the two moments mentioned above, it will be remembered that Eq. (2) was developed for a square knee with vertical stiffener extensions of the inner beam and column flanges as sketched in Fig. 13. Such vertical stiffeners are not

present in type 2 connections. However, the web material will act somewhat in the same capacity. Assuming the same conditions as were used in developing Eq. (2),

$$M_{h(b)} = \frac{wd^2 G\gamma_2}{(1-\frac{d}{L})} \quad \ldots\ldots\ldots\ldots\ldots\ldots (27)$$

Since

$$M_h = M_{h(a)} + M_{h(b)}$$

Then,

$$M_h = \gamma_2 \left[\frac{wd^2}{1-\frac{d}{L}} G + \frac{A_s dE}{\sqrt{2}} \right] \quad \ldots\ldots\ldots\ldots\ldots\ldots (28)$$

from which γ_2 may be obtained

The rotation β_2 due to bending of a type 2 connection is determined directly from Eq. (17). Similarly, the equation for rotation ϕ_r is identical with Eq. (18). Thus,

$$\theta_2 = \gamma_2 + \beta_2 + \phi_r$$

as determined from expressions (28), (17) and (18). For connection A in which an 8B13 section was used,

$$\theta_2 = (2.50 + 4.00 + 1.45) \times 10^{-6} \text{ rad/in-kip}$$

$$\theta_2 = 7.95 \times 10^{-6} \text{ rad/ in-kip.}$$

(II) TYPE 8B CONNECTIONS (VERTICAL AND DIAGONAL STIFFENERS)

For the type 8B connections with vertical stiffeners there appears to be less basis for an assumption regarding the transmission of flange forces, F_i, by the diagonal stiffener.

It will be assumed, instead, that the diagonal acts as if it increased the web area and were distributed uniformly over it. From Eq. (2),

$$\gamma_{8B} = \frac{\tau}{G} = \frac{1}{G} \cdot \frac{M_h}{d} \cdot \frac{(1 - \frac{d}{L})}{A_w'} \quad \ldots\ldots\ldots\ldots\ldots (29)$$

where

A_w' = the effective area of the web

$A_w' = A_w + A_s'$

A_s' = equivalent stiffener area

$$A_s' = \frac{\sqrt{2}\, d \times b_s \times t_s}{d} = \sqrt{2}\, b_s t_s$$

b_s = total width of stiffener

t_s = stiffener thickness

The bending rotation, β_{8B} and rolled-section rotations, ϕ_r, are computed from Eq. (17) and (18). Thus,

$$\theta_{8B} = (\gamma_{8B} + \beta_{8B} + \phi_r).$$

For connection L in which an 8B13 section was used, from Eqs. (29), (17) and (18),

$$\theta_{8B} = (2.51 + 4.00 + 1.45) \times 10^{-6} \text{ rad/in-kip}$$

$$\theta_{8B} = 7.96 \times 10^{-6} \text{ rad/in-kip}.$$

This relationship is plotted in Fig. 42.

It will be observed that this value is the same as that determined for the type 2 connection. Although computed on the basis of different assumptions, the calculation of rotation due to shear gave practically identical results.

2d. "Equivalent Length" Rotation Analysis:

In section II, "Requirements for Connections", it was mentioned that on the basis of minimum requirements the knee should be as stiff as an equivalent length of the rolled sections joined. Several "equivalent lengths" are shown in Fig. 9 (see Part I).

As is evident from the previous derivations, the calculation of elastic deformations by the simplest methods involves many assumptions. Another point to consider is that such calculations probably are not part of a routine office procedure. Further, calculations of deformation and moment distribution are based on the implied assumption that the knee is "rigid" at the point of intersection of neutral lines, but that the rest of the knee behaves as if it were part of the beam or column*. Thus, a calculation of the type now to be described is of importance.

(I) IDENTICAL MEMBERS

It will first be assumed that the moment is uniform along the knee length to be considered. Referring to Fig. 148a,

$$M_{AD} = M_{AB} = M_H = M_r$$

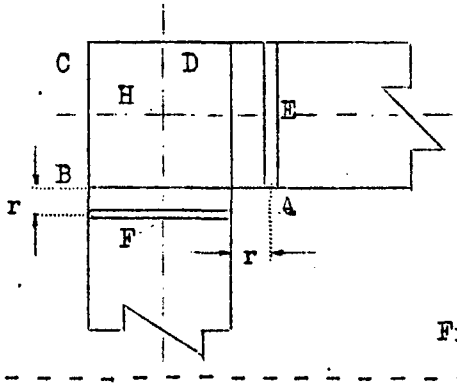

Fig. 148a

* See sketch "a", Appendix F, Part I.

Then

$$\phi_A = \phi \Delta L$$

where

$$\phi = \text{unit rotation, } \frac{M_r}{EI}$$

Then

$$\phi_A = \frac{M_h \left(1 - \frac{d}{2L}\right)}{EI} (d + 2r) \quad \ldots\ldots\ldots\ldots \quad (30)$$

For the 8B13 rolled shape used in this investigation, for an "r" distance of 1",

$$\phi_A = 7.06 \times 10^{-6} \text{ rad/in-kip.}$$

This relationship is plotted in Fig. 42 as indicated.

(II) DISSIMILAR MEMBERS ($d_1 \neq d_2$)

Following the same procedure as in the previous section and referring to Fig. 148b

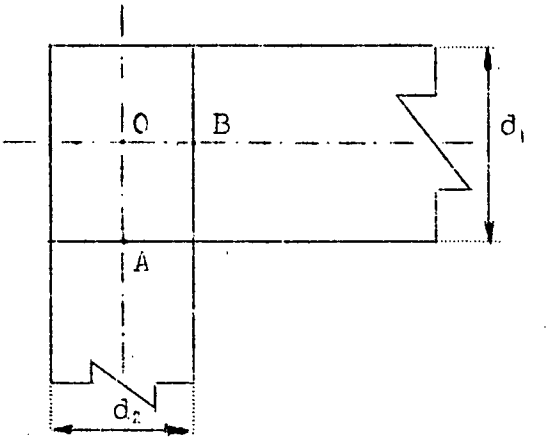

Fig. 148b

$$\phi_A = \beta_A + \phi_r$$

$$\beta_A = \int_o^B \frac{M_{r1}}{EI_1}\,dx + \int_o^A \frac{M_{r2}}{EI_2}\,dx$$

$$\beta_A = \frac{M_h}{2E}\left[\frac{d_2(1-\frac{d_2}{2L})}{I_1} + \frac{d_1(1-\frac{d_1}{2L})}{I_2}\right] \quad \ldots\ldots\ldots\ldots (31)$$

Evaluating β_A for connection P and adding the value ϕ_r determined from Eq. (22),

$$\phi_A = 3.053 \text{ rad/in-kip}$$

This elastic relationship is plotted in Fig. 38.

The deflection relationship in the elastic range will be discussed in the next section as a part of the plastic analysis.

II PLASTIC ANALYSIS

Yielding due to flexure alone will be discussed in this section. Thus only connections which do not yield due to shear force within the knee web will be considered. Although in the experimental program plastic deformation due to shear force occurred in one knee, it is recommended that means be taken in design to prevent such failure. Thus plastic deformation due to pure shear will not be considered. It will be assumed, then, that the knee area behaves as if it were a part of the beam and column.

The basis of the plastic deformation relationships is the moment angle-change curve, often referred to as the M-ϕ curve.

Methods for computing this function in the early plastic region were described by Luxion and Johnston[40]. Yang* has demonstrated the importance of the strain-hardening range and has described methods of computing the M-ϕ curve in this region.

In Fig. 102 the theoretical M-ϕ curve for a beam under pure bending is presented, the data being shown for the elastic and plastic stages only. Strain-hardening would not commence within the range of the curve.

In Fig. 102A are shown the theoretical and experimental M-ϕ relationships, the calculations being extended over a greater range. In these computations the results of coupon tests have been used, due account being taken for difference in material properties between the web and the flange. The upper yield point has been disregarded.

By way of summary, the equations for computing some of the critical points on the complete M-ϕ curve are as follows:

(1) Initial Yield

$$\left.\begin{aligned} M_1 &= \sigma_{yF} S \\ \phi_1 &= \frac{\sigma_{yF}}{E \frac{d}{2}} \end{aligned}\right\} \quad \ldots\ldots\ldots\ldots (32.1)$$

(2) Yielding has Penetrated to Bottom of Flange Fillet

$$\left.\begin{aligned} M_2 &= \frac{2}{3} \sigma_{yw} Z_2 + \sigma_{yF} (Z - Z_2) \\ \phi_2 &= \frac{\sigma_{yw}}{E_{y2}} \end{aligned}\right\} \quad \ldots\ldots\ldots\ldots (32.2)$$

---

* Dissertation by C.H. Yang "The Plastic Behavior of Continuous Beams", Lehigh University, 1951.

(3) Complete Plasticity ("plastic" hinge)

$$M_3 = \sigma_{yF}\,(Z-Z_2) + \sigma_{yw}Z_2 = M_P$$

$$\phi_3 = \infty \text{(neglecting strain-hardening)}$$

$$\phi_3 = \frac{\epsilon_s}{\frac{d}{2}} \text{ (considering strain-hardening)} \qquad \text{.... (32.3)}$$

(4) Strain-hardening has Penetrated to Bottom of Flange Fillet

$$M_4 = M_P + \frac{\sigma_4'}{(\frac{d}{2} - y_2)}\left[I - y_2\,(Z - \frac{Z_2}{3})\right]$$

$$\phi_4 = \frac{\epsilon_s}{y_2} \qquad \text{.... (32.4)}$$

(5) Strain-hardening has Penetrated to a Depth Corresponding to an Extreme Fibre Stress Equal to 130% σ_y

$$M_5 = M_P + \frac{\sigma_5'}{(\frac{d}{2} - y_5)}\left[I - y_5\,(Z - \frac{Z_5}{3})\right]$$

$$\phi_5 = \frac{\epsilon_s}{y_5} \qquad \text{.... (32.5)}$$

With several exceptions, the terms used in the above expressions have been previously defined or are defined in Appendix C.

$$Z_2 = w y_2^2$$

y_2 = distance from neutral axis to bottom of fillet

$$\sigma_4' = \epsilon_s\,(\frac{d}{2y_2} - 1)\,C$$

$$\sigma_5' = 0.30\,\sigma_y$$

$$y_5 = \frac{d}{2(1+\frac{.306 y}{C\epsilon_s})}$$

$$z_5 = w(y_5)^2$$

The influence of axial load (neglected entirely in the discussion) is to cause a reduction in the moment-carrying capacity as predicted by the simple plastic theory. This has been described by Baker(12) and also in Progress Report 2(75). As seen there, axial load does not reduce significantly the ultimate load-carrying capacity until the ratio of axial load to the buckling load exceeds about 0.10. Consequently, its influence will be neglected entirely. Such a ratio is not unusual in frames of the portal type.

1. ROTATION

In an earlier part of this report, on the basis of equivalent length of the rolled section, an expression for elastic rotation was developed (Eq. 30). This was derived from

$$\phi_A = \phi \cdot \Delta L$$

If it is assumed, as implied in the above expression, that the moment is uniform along the equivalent length being considered, then the M-ϕ curve (Fig. 102A) in the plastic and strain-hardening ranges may be used. The unit rotations determined from Fig. 102A (Eqs. 32) are merely multiplied by the equivalent length, ΔL. It is only necessary to correct the moment values by the ratio $\frac{M_h}{M_r}$, since the data of Fig. 102A corresponds to the moment M_r.

The results of this computation have been plotted in Fig. 42 (circles). The length over which the rotation was calculated has been assumed equal to the equivalent length of connection L. According to the above assumptions, strain-hardening would not commence until the rotation reached .044 radians, a value not within the range of the coordinates.

According to Fig. 143(a) it is evident that flange stresses decrease toward the outermost end of each stiffener. Thus, so far as the stiffeners are concerned, large deformations would not be expected upon reaching the flexural yield point.

If it were assumed that no inelastic rotation occurred within the knee, the M-ϕ_A relationship would be as shown by line m in Fig. 149 ($\phi_A = \phi \cdot \Delta L = \phi d$).

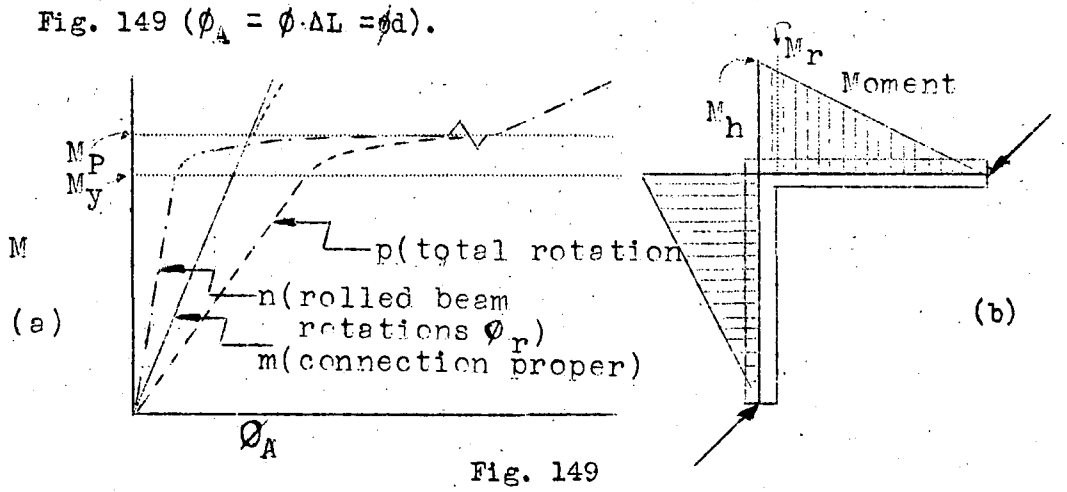

Fig. 149

Above M_y and in the region of M_P additional inelastic rotations would merely take place in the rolled section, the M-ϕ_A relationship of which is given by curve n ($\phi_A = \phi_r = \phi \times 2r$). Thus the M-$\phi_A$ curve of the complete connection is given by a summation of abscissae to give curve p.

The results of such a computation are also plotted on Fig. 42 (squares).

The same summation of incremental ϕ-values could be used in case the two members were dissimilar. By this method an $M-\phi_A$ curve could be obtained as shown in Fig. 150. Since yield occurred in connection P at a low load due to shear force this flexural calculation will not be carried further in this report.

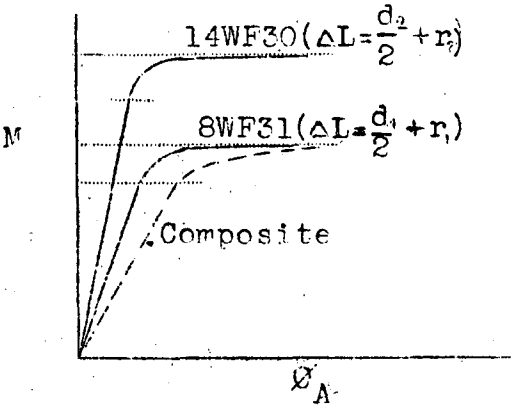

Fig. 150

2. DEFLECTION

Fig. 150

A number of methods of computing deflections beyond the elastic limit have been described by Yang in the dissertation previously mentioned. Only the simplest of these has been used here and the resulting moment-deflection relationship is plotted in Fig. 46. The points are computed in the following manner. Referring to Fig. 151,

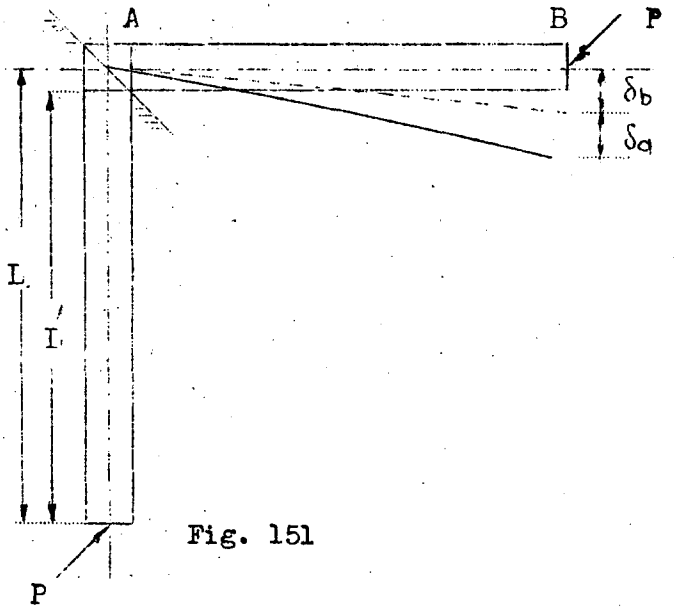

Fig. 151

$$\delta = \sqrt{2}\,(\delta_a + \delta_b) \quad \ldots\ldots\ldots\ldots\ldots\ldots \quad (33)$$

where

δ_a = deflection of the cantilever beam,

δ_b = additional deflection due to rotation of 1/2 of the knee computed about the intersection of the neutral lines of the members,

δ = deflection along the line of load P.

From Fig. 152,

$$\delta_a = y_1 + y_2 + y_3 \quad \ldots\ldots\ldots\ldots\ldots\ldots \quad (34)$$

where

$$\left.\begin{aligned} y_1 &= \frac{1}{CI}\left(\frac{1}{2}M_r x^2 - \frac{M_r x^3}{3L} - \frac{BZx^2}{2}\right) \\ y_2 &= \theta_x\,(L'-x) \\ y_3 &= \frac{M_A}{3L'EI}\,(L'-x)^3 \end{aligned}\right\} \quad \ldots\ldots \quad (34.1)$$

In the above expressions,

$$M_r = M_h\left(1 - \frac{d}{2L}\right),$$

$$x = L'\left(1 - \frac{M_P}{M_r}\right), \qquad L' = L - \frac{d}{2}$$

θ_x = slope at x as indicated in Fig. 152.

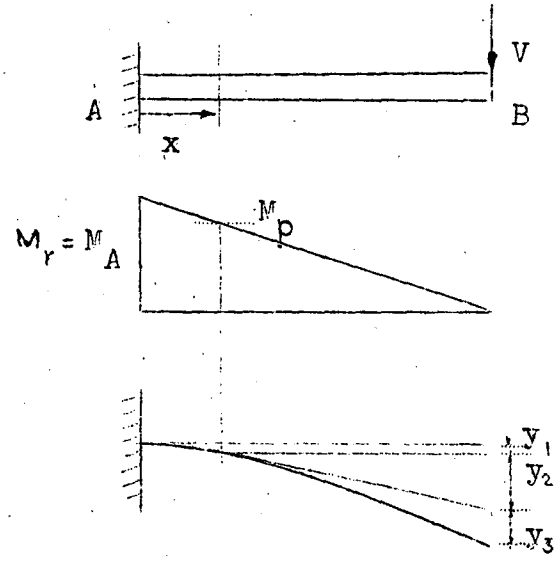

Fig. 152

$$\theta_x = \frac{1}{2CIM_r}\left[M_r^2 - M_p^2 - 2\,BZ(M_r - M_p)\right] \quad \ldots\ldots\ldots (34.2)$$

$$L' = L - \frac{d}{2}$$

The value δ_b is given from,

$$\delta_b = \frac{1}{2}\phi_A \times L \quad \ldots\ldots\ldots\ldots\ldots\ldots (35)$$

where ϕ_A is the rotation in the knee and is determined from the modified M-ϕ curve of Fig. 153 which is the basis for this particular method.

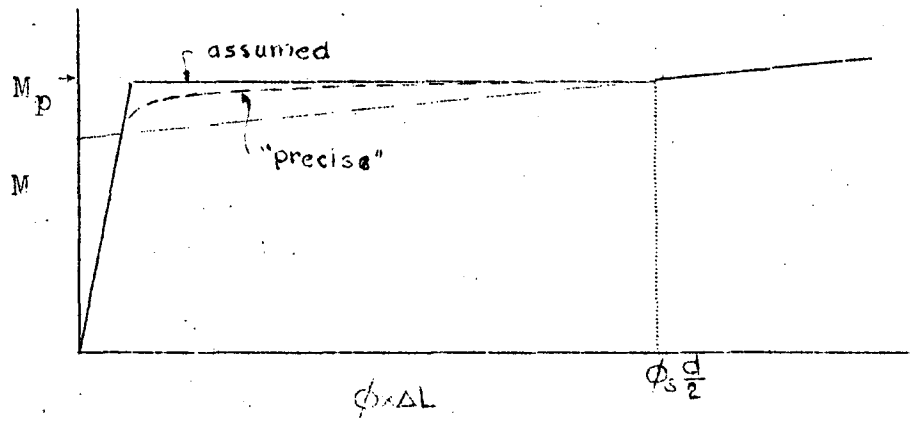

Fig. 153

The "equivalent length" concept is used. For $0 < M_r < M_p$

$$\phi_A = \frac{M_r d}{2EI} \quad \ldots\ldots\ldots\ldots\ldots\ldots (35.1)$$

and for $M_p < M_r < 1.3\ M_p$,

$$\phi_A = \left[\frac{M_r - BZ}{CI}\right]\frac{d}{2} \quad \ldots\ldots\ldots\ldots\ldots (35.2)$$

As is characteristic of this method for computing the load-deflection relationship the discrepancy between theory and experimental results is the greatest in the first part of the curve. This lack of agreement is accentuated in these tests by shear deformation, a portion of which is inelastic.

Note: The "Discussion" and "Summary" is to be included in Part III of this report to be distributed separately.

Appendix A

The calculations in this section were based on the following table:

TABLE OF PROPERTIES AND DIMENSIONS

Item	8B13		8WF31		14WF30		1/4" plate	
	Hand-book	Meas-ured	Hand-book	Meas-ured	Hand-book	Meas-ured	Hand-book	Meas-ured
σ_y(F)	33.0	41.8	33.0	39.2	33.0	38.18	33.0	39.1
σ_y(W)	33.0	47.1	33.0	--	33.0	40.7	--	--
I_x	39.5	42.07	109.7	115.55	289.6	285.75	--	--
A	3.83	3.993	9.12	9.314	8.81	8.874	--	--
S_x	9.88	10.42	27.4	28.39	41.8	41.56	--	--
w	.230	.237	.288	.296	.270	.277	--	--
t	.254	.266	.433	.438	.383	.340	.250	--
b	4.00	4.031	8.00	8.055	6.73	6.799	--	--
d	8.00	8.063	8.00	8.143	13.86	13.75	--	--
k	.563	.552	.813	--	.875	--	--	--
b/dt	7.9	--	2.31	--	5.37	--	--	--
L_u	6.0	--	21.5	--	9.5	--	--	--
ϵ_s	--	.0187	--	--	--	--	--	--
Z	11.38	12.006	30.366	32.910	47.090	46.212	--	--
$E_{(F)}$	30	30.1	--	--	30	--	30.0	30.07
$E_{(W)}$	30	28.0	30	--				
C	--	59.4	--	--	--	--	--	--
f	1.152	1.152	1.108	1.159	1.127	1.112	--	--
G	--	--	--	--	11.5	--	--	--
ρ	--	--	--	--	.30	--	--	--

NOTE: Nomenclature given in Appendix G of 205C.6A (Part I of Progress Report No. 4)

Appendix G

Welded Continuous Frames and Their Components

Nomenclature and Terminology

A = Area of cross-section.

B = σ axis intercept of extrapolated strain-hardening modulus line. Fig. h

C = Strain-hardening modulus = $\frac{d\sigma}{d\epsilon}$

f = Shape factor = $\frac{M_p}{M_y} = \frac{Z}{S}$

M = An applied moment

M_h = "Haunch" moment (connections)

M_p = "Hinge" value; full plastic moment; the ultimate moment that can be reached at a section according to the simple plastic theory. M_{ult} in Timoskenko. Collapse moment for a simple beam. Fig. b. $M_p = \sigma_y Z$.

M_{pc} = Collapse moment for a beam-column at a particular section. Fig. 4. The ultimate moment or collapse load of a column as modified by compression load.

M_r = Moment in a connection at junction of rolled beam & connection

M_s = Maximum moment of a simply-supported beam. Fig. o

M_y = Moment at which yield point is reached in flexure.. Fig. b. M_{yp} in Timoshenko.

M_{yc} = Same as M_y except modified for compression load. Fig. d.

P = An applied load.

P_{cr} = Useful column load. A load used as the "maximum column load" in design procedures. This might be P_t, P_o, P_{ult}

P_e = Euler buckling load.

P_p = Collapse load on a structure based on simple plastic theory.

P_t = Tangent Modulus Load...the load at which bending of a perfectly straight column may commence.

S = Section modulus, $\frac{I}{c}$. $S = \frac{M_y}{\sigma_y}$

tw = Web thickness.

Appendix G

Z = Plastic Modulus

= static moment of entire cross-section

$= \int_{y_1}^{y_2} y \, dA$ (Fig. 1) $= \frac{M_p}{\sigma_y}$

β = rotation in connection due to bending.

ϵ = Strain See Fig. h

γ = Rotation in connection due to shear.

ϕ = Rotation per unit length, Fig. m, n. or average unit rotation

$= \frac{\epsilon_1 + \epsilon_2}{2} \times \frac{1}{c}$

ΔL = Equivalent length of connection

θ = Measured angle change

σ = stress. σ_y = average yield point stress. Where used subscripts F & W refer to flange and web.

Actual stress-strain diagram: Fig. i

Buckling load: Maximum load carried by a member which fails due to instability. Fig. f, g.

Collapse moment: hinge value. Fig. k.

General yield: (Theoretical): $M_y = \sigma_y S$. (Experimental): significant decrease in slope of M-δ curve. Fig. k.

Hinge value: M_p (Plastic moment)

Idealized stress-strain diagram: Fig. h

Initial yield: Theoretical: Same as general yield.

Experimental (M-ϕ): M corresponding to $\phi = .0002/h/2$, Fig. j. This comes from the yield strength criterion for simple tension test.

Experimental (deflection): Point at which the straight line relation ceases. No rigorous definition is made. Select from curve (See Fig. k)

Local yield: Observation of first yield lines due to local effects This usually cannot be detected from a load-deformation diagram. Fig. k.

Appendix G

Modified hinge value: M_{pc}

Shape factor: $Z/S = f$

Simple plastic theory: According to this theory the formation of a plastic hinge is followed by further rotation under constant moment M_p without modification due to strain-hardening or instability.

Stiffness (rigidity): (Interchangeable) Moment divided by total rotation over an equivalent length, or moment divided by average unit rotation.

Yield Lines: Flaking of mill scale following formation of Luder's lines as revealed by whitewash.

Fig. a: Loading on Beam

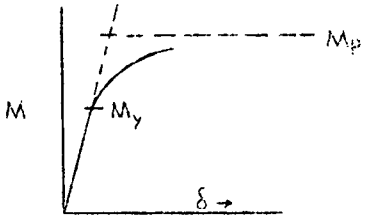

Fig. b: Moment - Deformation Diagram of Beam of Fig. a

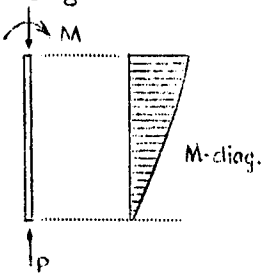

Fig. c: Loading on a Column

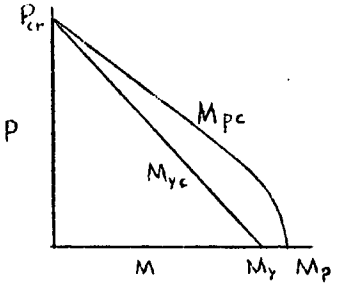

Fig. d: Typical Interaction Curve Showing Effect of Increase In Axial Load on Moment Capacity

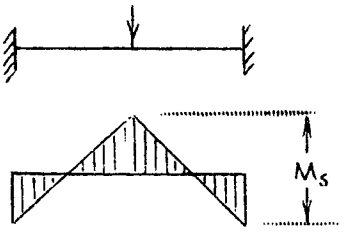

Fig. e: Typical Load and Moment Diagram

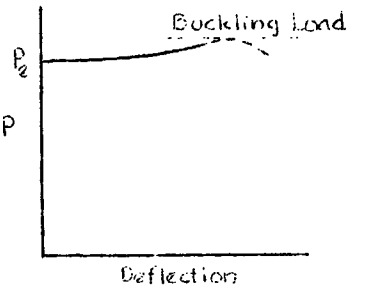

Fig. f: Column Deformation

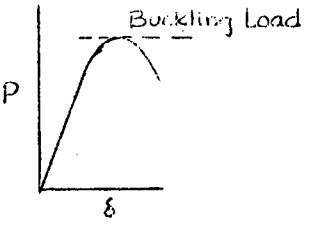

Fig. g: Eccentric Column

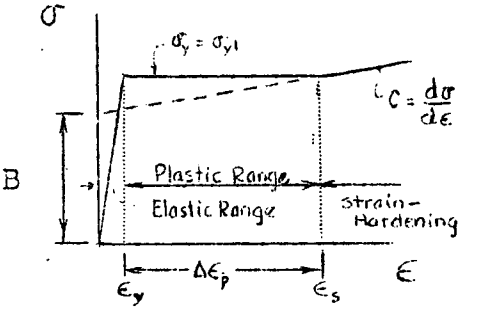

Fig. h: Idealized Stress-Strain Diagram

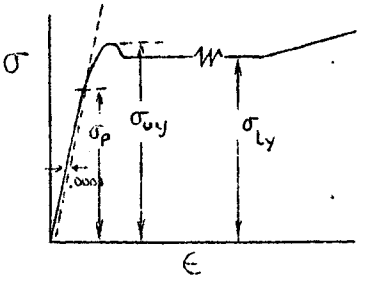

Fig. i: Actual or Typical Stress-Strain Diagram

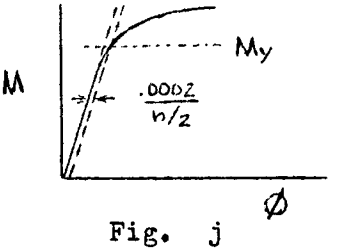

Fig. j

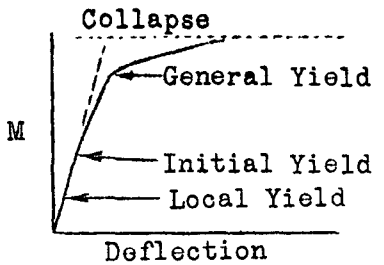

Fig. k: Experimental Curve

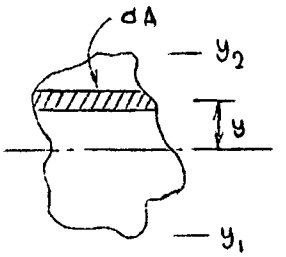

Fig. l

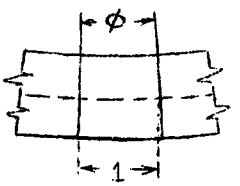

Fig. m

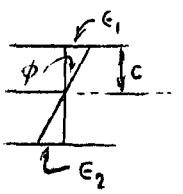

Fig. n

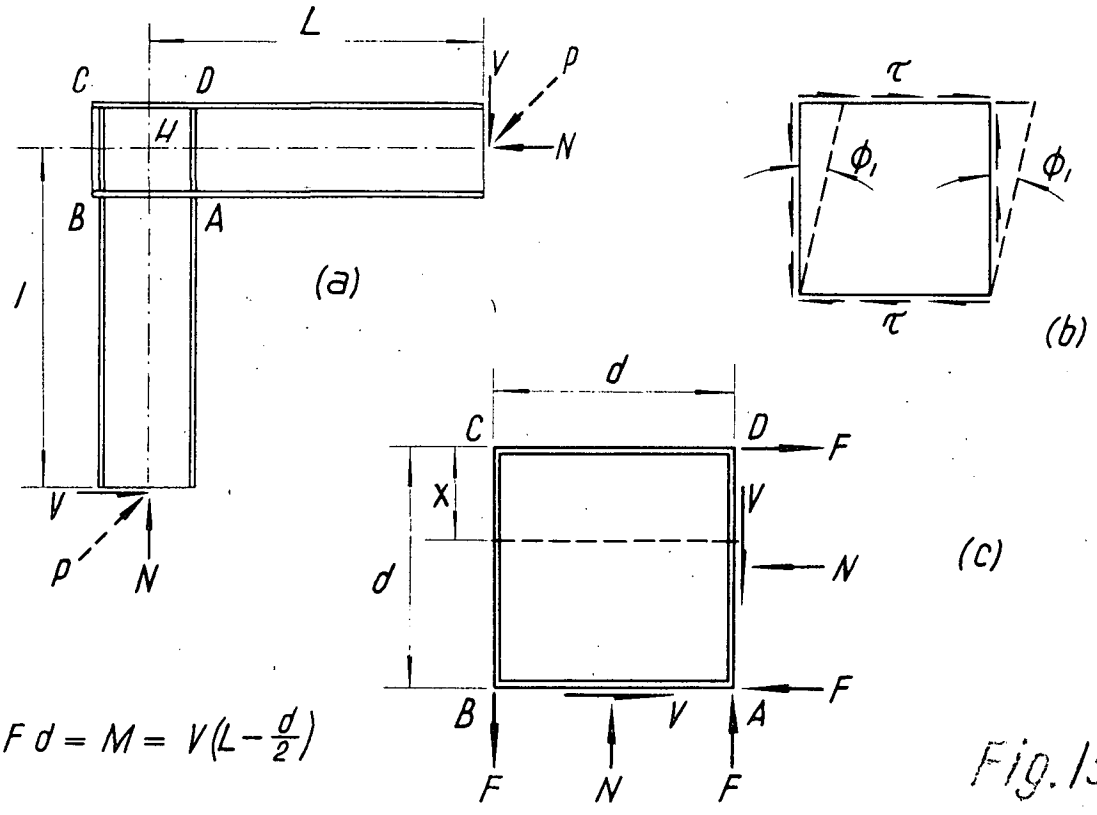

$$F\,d = M = V\left(L - \frac{d}{2}\right)$$

Fig. 13.

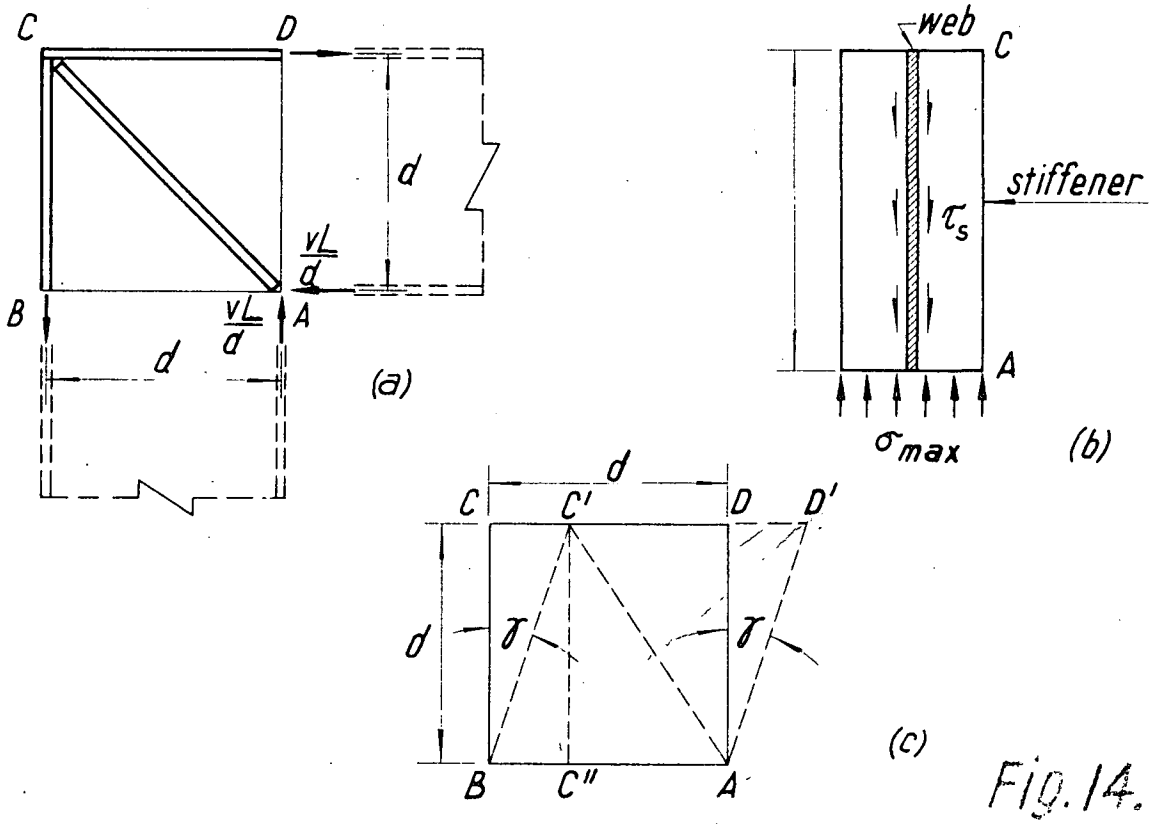

Fig. 14.

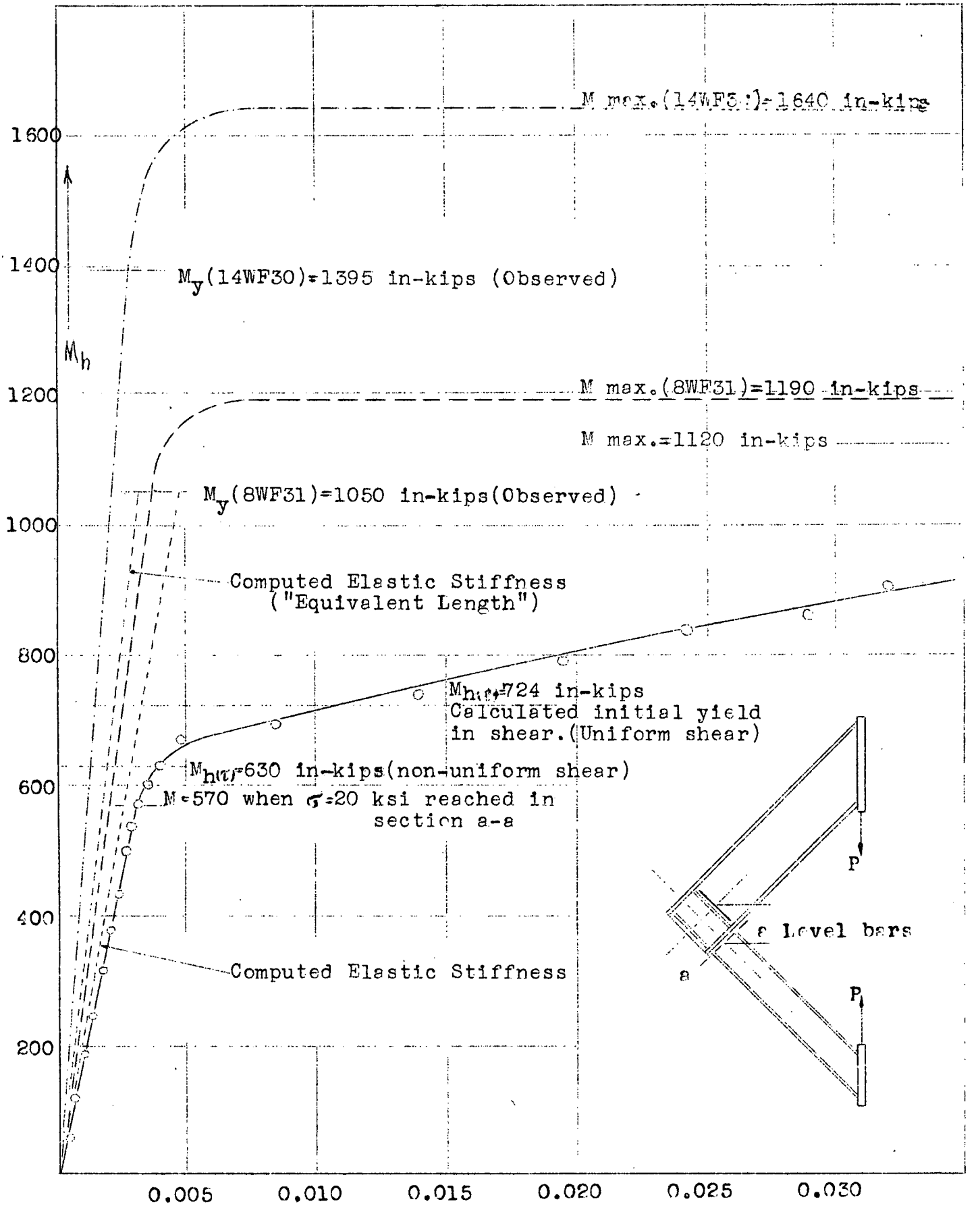

MOMENT - ROTATION CURVE. CONNECTION P, TYPE 7

Fig. 38

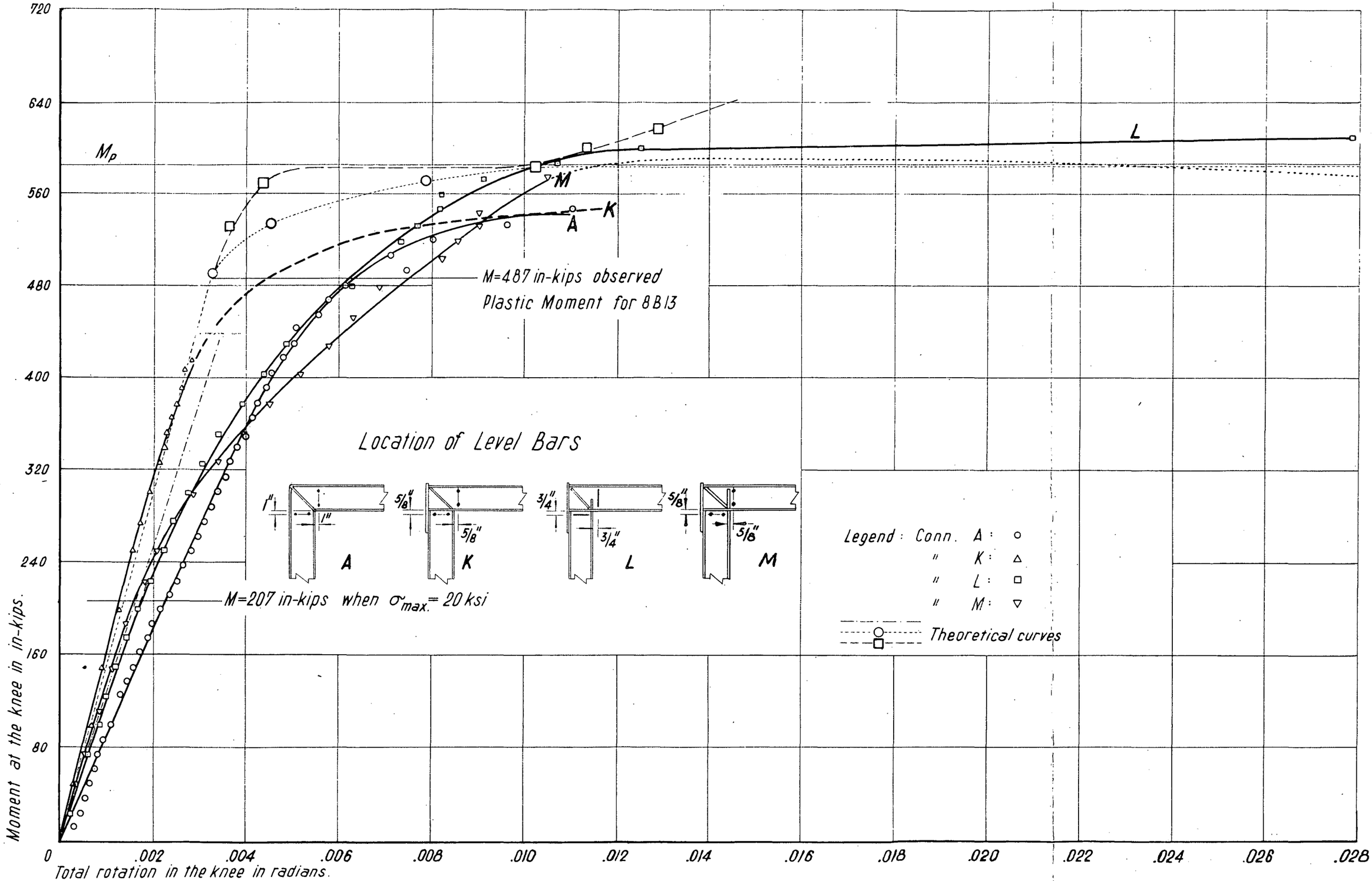

Moment–Rotation Curves for Connections A, K, L and M.

Fig. 42.

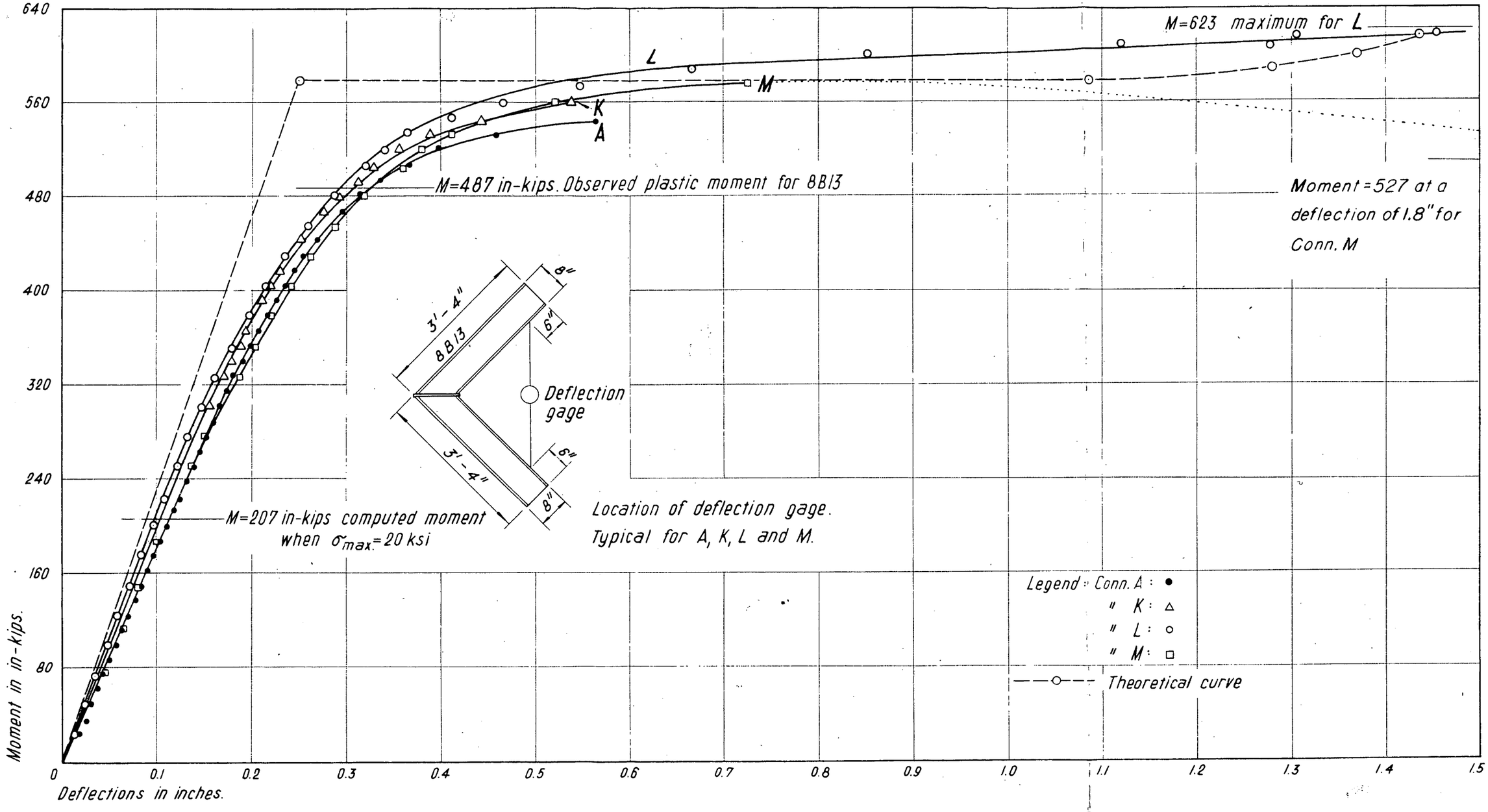

Fig. 46 Moment-Deflection Curves for Connections A, K, L and M.